

GEODESY

UDC 528.21 / 22

ALEXANDER N. MARCHENKO, S. S. PERII, Z. R. TARTACHYNSKA, A. P. BALIAN

Lviv Polytechnic National University, Institute of Geodesy, 6, Karpinskoho Str., Lviv, 79013, Ukraine,
e-mail: march@pancha.lviv.ua, periy_ss@ukr.net, ztartachynska@yahoo.com

<https://doi.org/10.23939/jgd2020.02.005>

TEMPORAL CHANGES IN THE EARTH'S TENSOR OF INERTIA AND THE 3D DENSITY MODEL BASED ON THE UT/CSR DATA

This study aims to derive the Earth's temporally varying Earth's tensor of inertia based on the dynamical ellipticity $H_D(t)$, the coefficients $\bar{C}_{2m}(t)$, $\bar{S}_{2m}(t)$ from UT/CSR data. They allow to find the time-varying Earth's mechanical and geometrical parameters during the following periods: (a) from 1976 to 2020 based on monthly and weekly solutions of the coefficient \bar{C}_{20} ; (b) from 1992 to 2020 based on monthly and weekly solutions of the non zero coefficients $\bar{A}_{20}(t)$, $\bar{A}_{22}(t)$ related to the principal axes of inertia, allowing to build models their long-term variations. Differences between \bar{C}_{20} and \bar{A}_{20} , given in various systems, represent the average value $\approx 2 \cdot 10^{-15}$, which is smaller than time variations of \bar{C}_{20} or \bar{A}_{20} , characterizing a high quality of UT/CSR solutions. Two models for the time-dependent dynamical ellipticity $H_D(t)$ were constructed using long-term variations for the zonal coefficient $\bar{A}_{20}(t)$ during the past 44 and 27.5 years. The approximate formulas for the time-dependent dynamical ellipticity $H_D(t)$ were provided by the additional estimation of each parameter of the Taylor series, fixing $H_D = 3.27379448 \times 10^{-3}$ at epoch $t_0 = \text{J2000}$ according to the IAU2000/2006 precession-nutation theory. The potential of the time-dependent gravitational quadrupole V_2 according to Maxwell theory was used to derive the new exact formulas for the orientation of the principal axes \bar{A} , \bar{B} , \bar{C} via location of the two quadrupole axes. Hence, the Earth's time-dependent mechanical and geometrical parameters, including the gravitational quadrupole, the principal axes and the principal moments of inertia were computed at each moment during the past 27.5 years from 1992 to 2020. However, their linear change in all the considered parameters is rather unclear because of their various behavior on different time-intervals including variations of a sign of the considered effects due to a jump in the time-series $\bar{C}_{20}(t)$ during the time-period 1998–2002. The Earth's 3D and 1D density models were constructed based on the restricted solution of the 3D Cartesian moments inside the ellipsoid of the revolution. They were derived with conditions to conserve the time-dependent gravitational potential from zero to second degree, the dynamical ellipticity, the polar flattening, basic radial jumps of density as sampled for the PREM model, and the long-term variations in space-time mass density distribution. It is important to note that in solving the inverse problem, the time dependence in the Earth's inertia tensor arises due to changes in the Earth's density, but does not depend on changes in its shape, which is confirmed by the corresponding equations where flattening is canceled.

Key words: Temporal change in principal axes and moments of inertia; Dynamical ellipticity; Gravitational quadrupole; Precession-Nutation theory.

Introduction

Processing of SLR (Satellite Laser Ranging) data led to precise information about a long time-series of the time-varying Earth's gravity field during the time-interval 1976–2020. Since 1983 the secular variation $\dot{J}_2 = -\sqrt{5} \cdot \dot{\bar{C}}_{20}$ in the normalized harmonic coefficient \bar{C}_{20} of the gravitational potential was derived by Yoder et al. (1983) with the simplest linear model

$$\bar{C}_{20}(t) = \bar{C}_{20} + \Delta\bar{C}_{20} = \bar{C}_{20} + \dot{\bar{C}}_{20}(t - t_0)$$

consisting of the time-independent part \bar{C}_{20} at epoch t_0 and the secular variation $\dot{\bar{C}}_{20}$. This model for the time-dependent coefficient \bar{C}_{20} was applied in various studies, e.g. Rubincam, 1984; Cheng et al., 1989; Schwintzer et al., 1991; Cheng et al., 2004; IERS Standards, 2010; Cheng et al., 2011; etc.

Contrary to the linear model Cheng et al., 2013 applied the enhanced approximation with the quadratic term additionally to the linear model for the $\bar{C}_{20}(t)$ time-series, during the time-interval from 1976 to 2011. Marchenko and Lopushansky (2018) used a similar approach for the period from 1976 to 2017 yr. and subinterval from 1992 to 2017 yr. It allowed revealing the long-term variations in $\bar{C}_{2m}(t)$, $\bar{S}_{2m}(t)$, and the dynamical ellipticity $H_D(t)$. According to Cheng et al., 2013 the linear model can be used successfully only on short time intervals. But a long time interval requires a choice of special modeling including probable fit by Fourier-Hermit series if the infinite interval is considered (Marchenko, 1998; Marchenko, Abrikosov, 2001).

Therefore, after 1983 yr. only the Earth gravitational potential is measured as time-dependent. The corresponding density distribution in the famous Newtonian integral for the gravitational potential should be considered also as time-dependent. The problem of the standard Earth's density model was formulated by the IAG in 1971. As a result, the well-known PREM model was developed by Dziewonski and Anderson (1981). The classical theory is given by Clairaut, Laplace, G. Darwin, Bullard (1954), Bullen (1975), Moritz (1990), etc. General discussion of different density distributions related to Clairaut, Williamson-Adams, and Poisson equations can be found in (Marchenko, 2000). The parameterization of the 1D density via the Gaussian radial profile is one of the possible solutions of the Williamson-Adams differential equation also given in (Marchenko, 2000). But the density parameterization has a special significance when the Earth's corresponds to a deformable body with a time-varying gravity field. Hence, all suitable geodetic, astronomical, and other data for 3D density models are valid in the following. They involve the 1D static radial profile (such as PREM), fundamental astronomical – geodetic parameters which describe the 3D static global density and its temporal variations with a space-time mass density distribution as the 4D density changes.

Traditionally, basic estimates of the normalized time-dependent $\bar{C}_{2m}(t)$, $\bar{S}_{2m}(t)$ series are obtained usually from the analysis of SLR observations of the following satellites: Starlette, Stella, Ajisai, LAGEOS-1, LAGEOS-2, BEC, GRACE, Larets, and LARES (Cheng and Ries, 2017) and recent $\bar{C}_{2m}(t)$, $\bar{S}_{2m}(t)$ lead to more accurate solutions. Furthermore, latest determinations of the astronomical dynamical ellipticity H_D are derived from the precession constant p_A and based on the non-rigid Earth's rotation theory (Dehant et al., 1999; Mathews et al., 2002; Capitaine et al. 2003; Fukushima, 2003; Bourda, Capitaine, 2004; Petit, Luzum, 2010; Liu,

Capitaine, 2017) which was adopted by IAU resolutions at the epoch J2000 (Capitaine et al. 2009). New values of H_D , including the older determination by Williams (1994), already contained the secular change $\dot{\bar{C}}_{20}$ in the frame of the linear model (Marchenko, Schwintzer, 2003; Bourda, Capitaine, 2004). So, $\bar{C}_{2m}(t)$, $\bar{S}_{2m}(t)$, and $H_D(t)$ allow accurate determination of the time-dependent Earth's principal axes, principal moments of inertia, and other fundamental parameters due to more stable determinations of H_D .

As the first step, this study aims to derive the Earth's time-evolving dynamical ellipticity $H_D(t)$, the orientation of the principal axes of inertia, and their evolution with time from the coefficients $\bar{C}_{2m}(t)$, $\bar{S}_{2m}(t)$. If the values $\bar{C}_{2m}(t)$, $\bar{S}_{2m}(t)$, and $H_D(t)$ are known for each moment the calculation of the principal axes and principal moments of inertia is carried out via the solution of the eigenvalue-eigenvector problem together with accuracy estimation by the error propagation (Marchenko, 2003; Marchenko and Schwintzer, 2003). Hence, closed exact formulas for the eigenvalue-eigenvector problem can be found in both above mentioned articles and in the following papers (Chen, Shen, 2010; Chen, et al., 2015).

It is crucial to clarify that literature sources presented us only one recommended value of $H_D = 3.27379448 \times 10^{-3}$ at epoch J2000 according to the IAU 2000/2006 precession-nutation theory (Capitan, et al., 2009) instead of a series of the time-dependent ellipticity $H_D(t)$. As a result, the building of a suitable model for the time-dependent $H_D(t)$ is required. This problem can be solved approximately with the additional condition to conserve changes in the trace of the inertial tensor. It is possible, to compute time-dependent components of inertial tensor and other associated parameters if the model for $H_D(t)$ becomes established (Marchenko and Lopushansky, 2018). Thus, modeling beforehand the long-term variations in $H_D(t)$ is significant with $H_D = 3.27379448 \times 10^{-3}$ fixed at epoch J2000 based on the linear and quadratic terms. Components of the Earth's inertial tensor are derived from $\bar{C}_{2m}(t)$, $\bar{S}_{2m}(t)$, and $H_D(t)$ at each moment t . These $\bar{C}_{2m}(t)$, $\bar{S}_{2m}(t)$ also allow to find the potential of the gravitational quadrupole (Marchenko, 1979) having important parameters that are independent relating to the rotation of the adopted reference frame. Thus, they represent the invariant characteristics of the gravitational field which are dependent on time only.

Therefore, this study focuses on 1) the verification of previous formulas for modeling of the time-dependent $H_D(t)$ with $H_D = 3.27379448 \times 10^{-3}$ fixed at epoch $t_0 = \text{J2000}$; 2) the derivation of the new exact formulas for the orientation of the principal axes \bar{A} , \bar{B} , \bar{C} through the location of the two quadrupole axes; 3) the revealing of the long-term changes from monthly UT/CSR solutions of \bar{C}_{20} from 1976 to 2020; 4) the detection of long-term variations from weekly and monthly UT/CSR solutions of non zero $\bar{A}_{20}(t)$, $\bar{A}_{22}(t)$ related to the principal axes system over the time interval from 1992 to 2020; 5) the construction of the time-dependent model of $H_D(t)$ using $\bar{A}_{20}(t)$ during the past 27.5 years; 6) the calculation of the principal axes $\bar{A}(t)$, $\bar{B}(t)$, $\bar{C}(t)$, the principal moments $A(t)$, $B(t)$, $C(t)$ of inertia and other fundamental parameters; 7) the determination of the Earth's 3D density model and the corresponding long-term variations in space-time mass density distribution.

Modeling the Earth's time-dependence dynamical ellipticity

In the first step the transformation of the vector $\mathbf{g}(t) = [\bar{C}_{20}(t); \bar{C}_{21}(t); \bar{S}_{21}(t); \bar{C}_{22}(t); \bar{S}_{22}(t)]^T$ of $\bar{C}_{2m}(t)$, $\bar{S}_{2m}(t)$, defined in the Earth's-fixed geocentric coordinate system X, Y, Z , to the vector $\tilde{\mathbf{g}}(t) = [\bar{A}_{20}(t), 0, 0, \bar{A}_{22}(t), 0]^T$ of the non zero harmonic coefficients $\bar{A}_{20}(t)$, $\bar{A}_{22}(t)$ in the instant coordinate system of the principal axes of inertia $\bar{A}(t)$, $\bar{B}(t)$, $\bar{C}(t)$ is applied. Assuming initial data to consist of the vector $\mathbf{g}(t)$ for each moment of time $t = t_k$ ($k = 1, 2, \dots, q$) with the variance-covariance matrix, we will use the closed formulas of the eigenvalue-eigenvector problem given in Marchenko and Schwintzer (2003) for the determination of $\bar{A}_{20}(t)$, $\bar{A}_{22}(t)$ in the principal axes system. By involving the dynamical ellipticity $H_D(t)$ we can find the normalized by the factor $1/Ma^2$ time-dependent principal moments of inertia $A(t)$, $B(t)$, and $C(t)$ (under the condition $M = \text{const}$):

$$H_D(t) = (2C(t) - A(t) - B(t))/2C(t) \Leftrightarrow C(t) = -\sqrt{5}\bar{A}_{20}(t)/H_D(t), \quad (1a)$$

$$A(t) = \sqrt{5}\bar{A}_{20}(t)(1 - 1/H_D(t)) - \sqrt{15}\bar{A}_{22}(t)/3, \quad (1b)$$

$$B(t) = \sqrt{5}\bar{A}_{20}(t)(1 - 1/H_D(t)) + \sqrt{15}\bar{A}_{22}(t)/3. \quad (1c)$$

The orientation of the principal axes in the (X, Y, Z)-frame is based on the new formulas (16), using $\bar{C}_{2m}(t)$, $\bar{S}_{2m}(t)$ without H_D . The H_D -values are given by (Williams, 1994; Mathews et al., 2002; Fukushima, 2003; Capitane et al., 2003) have a small differences between the adopted $H_D = 0.0032737945$ according to IAU2000/2006 Precession-Nutation model (see, Petit, Luzum, 2010).

To transform the associated quantities from different p_A to the common value $p_A = 50.2879225''/\text{yr}$. the relationship $\delta H_D = 6.4947 \cdot 10^{-7} \delta p_A$ of Souchay and Kinoshita (1996) can be applied. These H_D have much better accordance with the IAU 2000/2006 dynamical ellipticity H_D .

The calculation of $A(t)$, $B(t)$, $C(t)$, and the trace $\text{Tr}(\mathbf{I}(t))$ of the tensor of inertia are straightforward

$$\text{Tr}(\mathbf{I}(t)) = A(t) + B(t) + C(t) = 3I_m(t) = \sqrt{5}\bar{A}_{20}(t)(2 - 3/H_D(t))$$

via Eqs. (1) for each given moment of $t = t_k$. From this we get a direct dependence of $A(t)$, $B(t)$, $C(t)$, $\text{Tr}(\mathbf{I}(t))$, and the mean moment $I_m(t)$ of

inertia on the treatment through $\bar{C}_{20}(t)$ of the permanent tide in $\bar{A}_{20}(t) \approx \bar{C}_{20}$, $\bar{A}_{22}(t)$ represented by the following equations

$$-\sqrt{5}\bar{A}_{20}(t) = (2C(t) - A(t) - B(t))/2, \quad 2\sqrt{15}\bar{A}_{22}(t)/3 = B(t) - A(t). \quad (2)$$

The difference $B(t) - A(t)$ is also slightly dependent on a tide system because $\bar{C}_{20}(t)$ enters

into the calculation of the coefficient $\bar{A}_{22}(t)$. Hereafter it is assumed that the $\bar{A}_{20}(t)$, $\bar{A}_{22}(t)$, and

$H_D(t)$ values are related to the zero-frequency tide system (Groten, 2000). However the UT/CSR $\bar{C}_{2m}(t)$, $\bar{S}_{2m}(t)$ – estimates are based on the background gravity model including the solid earth and ocean tides, the solid earth and ocean pole tides, and other effects. To separate various influences for the filtering only components of the time-dependent gravity field we need to provide an additional study. But the computation of long-term variations only based on the initial $\bar{C}_{2m}(t)$, $\bar{S}_{2m}(t)$ was assessed to be significant.

If the gravity field of the elastic celestial body is variable, this produces small changes for all parameters in Eq. (3). From the formula (3), taking into account that the additional condition for the

$$d\text{Tr}(\mathbf{I}(t)) = dA(t) + dB(t) + dC(t) = d[3I_m(t)] = 0, \Leftrightarrow dA(t) = dB(t) = -dC(t)/2, \quad (4)$$

one gets for the secular change in $H_D(t)$, after Taylor expansion of Eq. (3):

$$H_D(t) = H_D|_{t=t_0} + dH_D = H_D|_{t=t_0} + \left. \frac{dH_D(t)}{dt} \right|_{t=t_0} (t-t_0) + \frac{1}{2} \left. \frac{d^2H_D(t)}{dt^2} \right|_{t=t_0} (t-t_0)^2 + \dots, \quad (5)$$

where the first and second derivatives can be found in the following way

$$\left. \frac{dH_D(t)}{dt} \right|_{t=t_0} = -\frac{\sqrt{5}\dot{\bar{A}}_{20}}{C}, \quad \left. \frac{d^2H_D(t)}{dt^2} \right|_{t=t_0} = -\frac{\sqrt{5}\ddot{\bar{A}}_{20}}{C}, \quad \dot{C}(t) = \frac{dC(t)}{dt}, \quad \ddot{C}(t) = \frac{d^2C(t)}{dt^2}, \quad (6)$$

where all insignificant terms were omitted due to the computed value of $\dot{\bar{A}}_{20} = -7.461 \cdot 10^{-12} \text{ yr}^{-1}$ ($\frac{d\dot{\bar{A}}_{20}}{dt} = \ddot{\bar{A}}_{20}$) for our interval from 1992 to 2020 yr. According to Eq.(2) and Eq. (4) (Burša, et al., 2008; Marchenko, 2009a) the linear change \dot{C} at epoch J2000 can be calculated as $\dot{C} = 1.112 \cdot 10^{-11} \text{ yr}^{-1}$. Moreover, the derivatives \ddot{C} and $\ddot{\bar{A}}_{20}$ ($\frac{d^2\dot{\bar{A}}_{20}}{dt^2} = \ddot{\bar{A}}_{20}$) at least smaller or may have values of the same order as \dot{C} and $\dot{\bar{A}}_{20}$. Hence four terms in the full expressions for derivatives $\frac{dH_D}{dt}$ and $\frac{d^2H_D}{dt^2}$, having magnitude $\sim 10^{-15}$, are insignificant in comparison with \dot{C} , $\dot{\bar{A}}_{20}$, and $\ddot{\bar{A}}_{20}$ that leads to the final solution

$$d\bar{A}_{20}(t) = \left[\dot{\bar{A}}_{20}(t-t_0) + \ddot{\bar{A}}_{20}(t-t_0)^2 \right], \quad (7)$$

where $d\bar{A}_{20}(t)$ is nothing else but the long-term change (linear and quadratic) in the time-dependent zonal harmonic coefficient of degree 2 given in the principal axes system.

Thus, after the choice of the long periodic model for $d\bar{A}_{20}(t)$ we get the required solution with respect

Let us derive the variations of the dynamical ellipticity $H_D(t)$ from $\bar{A}_{20}(t)$, $\bar{A}_{22}(t)$ time-series and IAU2000/2006 dynamical ellipticity $H_D = 0.0032737945$ fixed at epoch J2000. The approximate solution of the problem is possible because $\bar{A}_{20}(t)$, $\bar{A}_{22}(t)$ can be found separately from the vector $\mathbf{g}(t)$. Furthermore, the expression (1a) can be written as

$$H_D(t) = -\frac{\sqrt{5}\bar{A}_{20}(t)}{C(t)}. \quad (3)$$

trace $\text{Tr}(\mathbf{I}(t)) = \text{const}$ (Rochester and Smylie, 1974) “as zonal forces do not change the revolution shape of the body” (Melchior, 1978; Souchay and Folgueira, 1998):

to the epoch $t_0 = 2000$ based on the following relationship

$$H_D(t) = H_D|_{t=t_0} - \frac{\sqrt{5}}{C} \cdot \left(\dot{\bar{A}}_{20}(t-t_0) + \ddot{\bar{A}}_{20}(t-t_0)^2 \right) \quad (8)$$

if both linear and the quadratic components of \bar{A}_{20} are taking into account and C is related to the epoch $t_0 = 2000$. As a result, Eq. (8) by definition can represent the only long-term variation of $H_D(t)$ because it was derived via estimates of the derivatives \dot{C} , $\dot{\bar{A}}_{20}$ and \ddot{C} , $\ddot{\bar{A}}_{20}$.

Models for C_{20} and the dynamical ellipticity

From the transformation of the vector \mathbf{g} known in (X, Y, Z) , to the vector $\tilde{\mathbf{g}}$, given in the principal axes $(\bar{A}, \bar{B}, \bar{C})$, we can determine \bar{A}_{20} at epoch and the differences between \bar{C}_{20} and \bar{A}_{20} . In this case, such differences can be based on the UT/CSR solutions for the time-dependent coefficients $\bar{C}_{2m}(t)$, $\bar{S}_{2m}(t)$ during the period from 1992 to 2020. After transformation to $\bar{A}_{20}(t)$, $\bar{A}_{22}(t)$ we get the average difference $(\bar{C}_{20} - \bar{A}_{20}) \approx 2 \cdot 10^{-15}$

smaller than UT/CSR long-term variations. A value of difference $\approx 2 \cdot 10^{-15}$ corresponds to the non-zero invariant $I_1 \approx 10^{-15}$ according to Lambek's formulas (Lambek, 1971; Marchenko, 2009a). There are different models chosen for time-dependent change of

$$\bar{A}_{20} = \bar{A}_{20}^0 + \dot{\bar{A}}_{20}(t-t_0) + \ddot{\bar{A}}_{20}(t-t_0)^2 + A_a \cos\left(\frac{2\pi}{P_a}(t-t_0) - \{\phi_a\}\right), \quad (9)$$

where \bar{A}_{20}^0 are the adopted value of \bar{A}_{20} at reference epoch t_0 ; $\dot{\bar{A}}_{20}$, $\ddot{\bar{A}}_{20}$ are the parameters of long-term variations in \bar{A}_{20} , which are valid at the vicinity of t_0 ; (A_a, ϕ_a) are the components of the annual variations with the period P_a .

the coefficient \bar{A}_{20} (for example, Cheng et al, 2011; Cheng et al, 2013; etc). Here one starts from the \bar{A}_{20} model taken from the paper (Marchenko and Lopushansky, 2018) and representing the change in time as

Fig. 1 ($\bar{C}_{20}(t)$ during the period from 1976 to 2020) and Fig. 2 ($\bar{A}_{20}(t)$ during the interval from 1992 to 2020) illustrate the aforementioned UT/CSR time series of \bar{C}_{20} , which were modeled by polynomials up to the second degree simultaneously with Fourier series. Most stable solutions were obtained in both cases including only an annual period.

Table 1

Coefficients for the polynomial representation of the long periodic trend for \bar{A}_{20} (blue line) in the form $\bar{A}_{20} = \bar{A}_{20}^0 + \dot{\bar{A}}_{20}(t-t_0) + \ddot{\bar{A}}_{20}(t-t_0)^2$ at epoch J2000 (see, Eq. (9), Fig. 1)

Solution	\bar{A}_{20}^0	$\dot{\bar{A}}_{20}$ [yr ⁻¹]	$\ddot{\bar{A}}_{20}$ [yr ⁻²]
Cheng, et al., 2013	-484.169453E-06	0.27E-11	-0.40E-12
Marchenko, Lopushansky, 2018, I	-484.1694554194E-06	0.1166E-11	-0.4844E-12
Marchenko, Lopushansky, 2018, II	-484.1695458067E-06	-0.1001E-10	0.3659E-12
This study, I (1976–2020)	-484.1695331837E-06	-0.2559E-11	-0.3792E-12
This study, II (1992–2020)	-484.1695422666E-06	-0.1026E-10	0.2960E-12
This study, III (1992–2020)	-484.1695355089E-06	-0.7461E-11	–

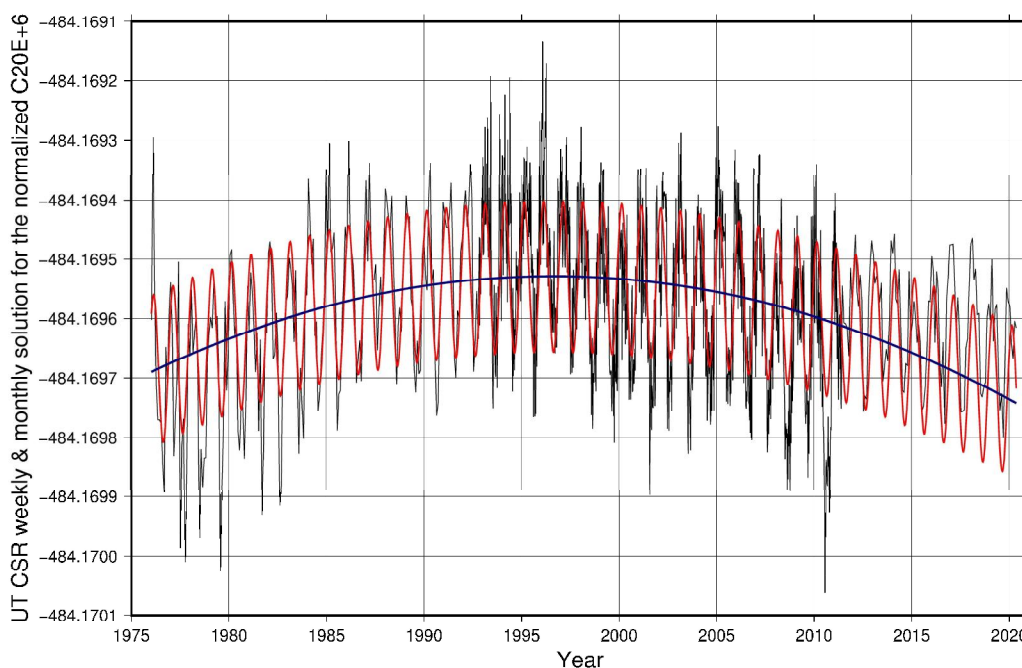


Fig. 1. UT/CSR series of \bar{C}_{20} (period from 1976 yr to 2020 yr. – black line) where the long-term variations fixed at epoch J2000 were modeled by polynomials up to 2nd degree (blue line) (solution I in Table 1) simultaneously with Fourier series using annual period (red line)

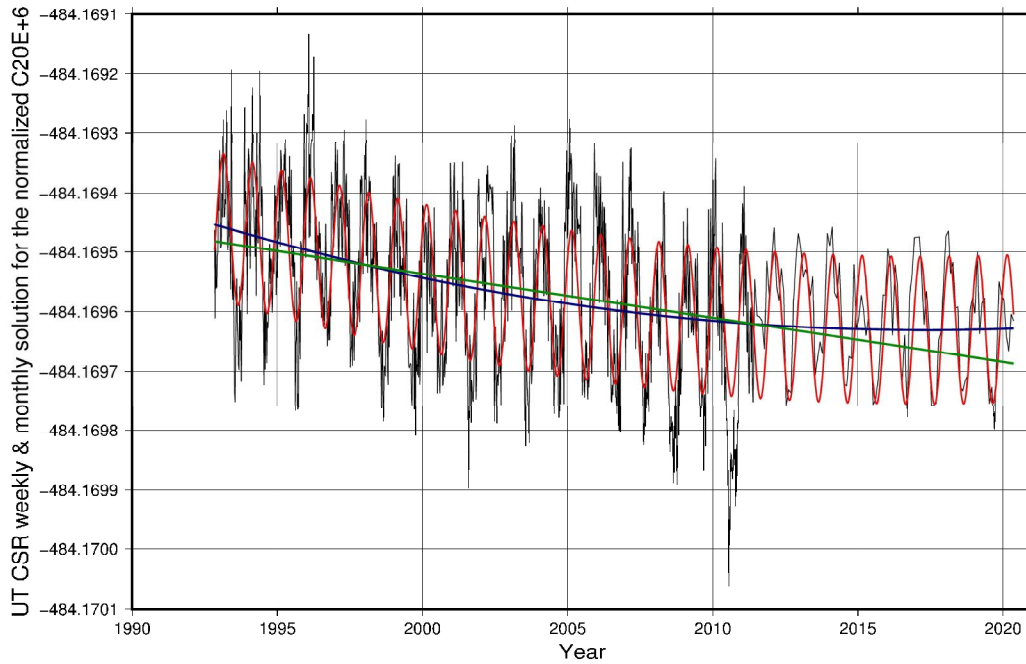


Fig. 2. UT/CSR time series of \bar{A}_{20} (period from 1992 to 2020 yr. – black line) where the long-term variation fixed at epoch J2000 was modeled by polynomials up to 2nd degree (blue line) simultaneously with Fourier series using annual period (red line) (solution II in Table 1). The linear model is shown in green (solution III in Table 1)

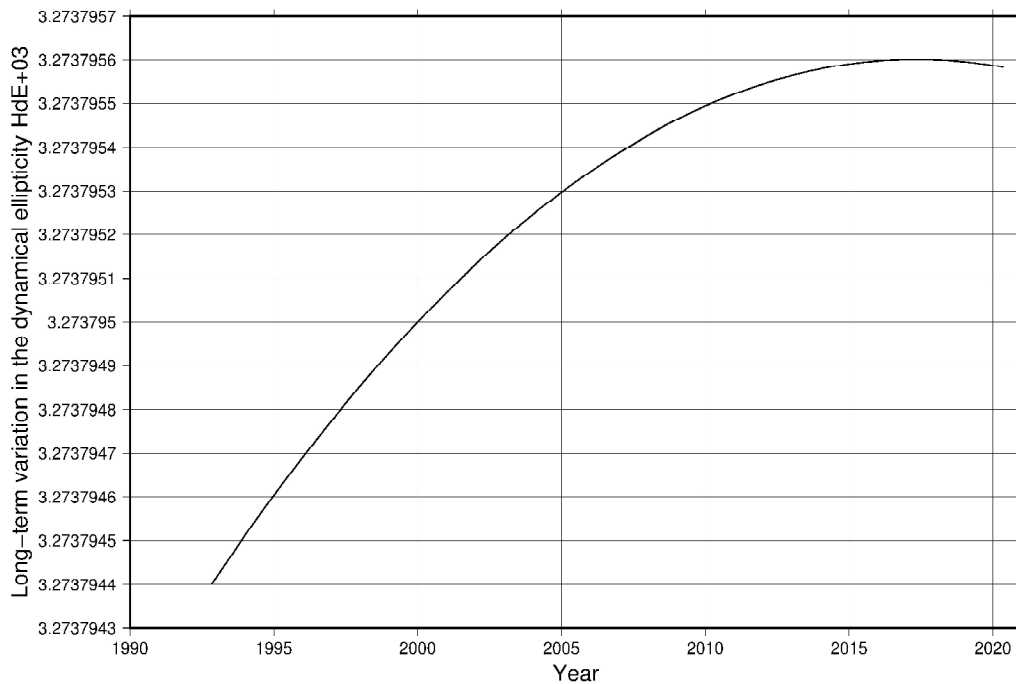


Fig. 3. Long-term variations (solid line) in the astronomical dynamical ellipticity H_D modeled according to Eq. (8) and Solution II model with $t_0 = J2000$

Table 1 illustrates the obtained models and the following result: more than three years additional $\bar{C}_{20}(t)$ coefficients from SLR data lead in this study to a small change in the long-term variations, taking into account the comparison with

(Marchenko et. al., 2018) during the time-interval 1992–2020.

On the contrary, we get large differences between (Cheng, et al., 2013; Marchenko et. al., 2018) results and this Solution I during the time-intervals (1976–2011) and (1976–2020) due to

longer periods of $\bar{C}_{2m}(t)$, $\bar{S}_{2m}(t)$, various initial data, and different approaches to data processing.

This leads to the idea to use the linear splines for better modeling of time-dependent parameters using suitable short intervals because the direct determination of $H_D(t)$ from observation is not found in the literature sources.

Obviously spline functions of the degree 2 or 3 will give a better quality of fitting, but in this case the approximation requires the necessity of estimation of the time series $H_D(t)$.

$$\mathbf{H} = \tilde{M}_2 \left[\frac{3}{2} (\mathbf{h}_1 \mathbf{h}_1^T + \mathbf{h}_2 \mathbf{h}_2^T) - \cos \tilde{\gamma} \cdot \mathbf{I} \right], \quad \tilde{\mathbf{H}} = \tilde{M}_2 \begin{pmatrix} \frac{3 + \cos \tilde{\gamma}}{2} & 0 & 0 \\ 0 & -\cos \tilde{\gamma} & 0 \\ 0 & 0 & -\frac{3 - \cos \tilde{\gamma}}{2} \end{pmatrix}, \quad (11)$$

are defined in the Earth's-fixed coordinate system (X, Y, Z) and in the principal axes of inertia $(\bar{A}, \bar{B}, \bar{C})$, respectively; \mathbf{r}^T and $\tilde{\mathbf{r}}^T$ are the Cartesian vectors of coordinates corresponding to these systems; GM is the product of the gravitational constant G and the planet's mass M ; a is the semi-major axis of the ellipsoid of revolution; r is the distance from the origin to the

Orientation of the principal axes through the gravitational quadrupole parameters

In addition to the formulas (1) we will use the second degree potential with the harmonic coefficients (C_{2m}, S_{2m}) which can be considered with other parameters as the potential of the Earth's gravitational quadrupole written in the identical Maxwell-Gauss form.

From the preceding studies (Maxwell, 1881; Marchenko, 1979; Marchenko, 1998) we get

$$V_2 = \frac{\sqrt{15} GMa^2}{2 r^5} \mathbf{r}^T \mathbf{H} \mathbf{r} = \frac{\sqrt{15} GMa^2}{2 r^5} \tilde{\mathbf{r}}^T \tilde{\mathbf{H}} \tilde{\mathbf{r}}, \quad (10)$$

where the matrices \mathbf{H} and $\tilde{\mathbf{H}}$:

current point; \mathbf{I} is the unit (3×3) matrix; $\mathbf{h}_1 = \mathbf{h}_1(l_1, m_1, n_1)$ and $\mathbf{h}_2 = \mathbf{h}_2(l_2, m_2, n_2)$ are the unit axial vectors corresponding to the quadrupole axes with the angle $\tilde{\gamma}$ between \mathbf{h}_1 and \mathbf{h}_2 ; \tilde{M}_2 is the normalized quadrupole moment M_2 , which is always positive by definition. Thus we get

$$M_2 > 0, \quad (\mathbf{h}_1 \cdot \mathbf{h}_1) = 1, \quad (\mathbf{h}_2 \cdot \mathbf{h}_2) = 1, \quad (\mathbf{h}_1 \cdot \mathbf{h}_2) = \cos \tilde{\gamma}, \quad (12)$$

$$M_2 = 2A_{22} - A_{20}, \quad \tilde{M}_2 = \frac{M_2}{\sqrt{15}} = \frac{\bar{A}_{22} - \sqrt{3}\bar{A}_{20}}{3}, \quad \cos \tilde{\gamma} = \frac{3\bar{A}_{22} + \sqrt{3}\bar{A}_{20}}{\bar{A}_{22} - \sqrt{3}\bar{A}_{20}}. \quad (13)$$

It is easily seen that the location of \mathbf{h}_1 and \mathbf{h}_2 will be always in the plane of the principal axes \bar{A} and \bar{C} . The axis \bar{A} is nothing else but the bisector of

the angle $\tilde{\gamma}$ and the axis \bar{C} is the bisector of the angle $\pi - \tilde{\gamma}$. Then we define two vectors coincided with the axes \bar{A} and \bar{C} :

$$\mathbf{a} = (\mathbf{h}_1 + \mathbf{h}_2)/2, \quad \mathbf{c} = (\mathbf{h}_1 - \mathbf{h}_2)/2, \quad \Rightarrow \quad \mathbf{h}_1 = \mathbf{a} + \mathbf{c}, \quad \mathbf{h}_2 = \mathbf{a} - \mathbf{c}, \quad (14)$$

and after some simple algebra we get their Euclidean norms in terms of A, B, C :

$$\|\mathbf{a}\|^2 = (\mathbf{a} \cdot \mathbf{a}) = \cos^2 \frac{\tilde{\gamma}}{2} = \frac{B - A}{C - A}, \quad \|\mathbf{c}\|^2 = (\mathbf{c} \cdot \mathbf{c}) = \sin^2 \frac{\tilde{\gamma}}{2} = \frac{C - B}{C - A}. \quad (15)$$

Eigenvectors or the principal axes are found as the solution of the homogeneous system of linear algebraic equations based on the matrix \mathbf{H} with the following resulting expressions

$$\left. \begin{aligned} u_A &= \pm \frac{l_1 + l_2}{2 \cdot \|\mathbf{a}\|}, & v_A &= \pm \frac{m_1 + m_2}{2 \cdot \|\mathbf{a}\|}, & w_A &= \pm \frac{n_1 + n_2}{2 \cdot \|\mathbf{a}\|}, \\ u_B &= \pm \frac{m_1 n_2 - m_2 n_1}{2 \cdot \|\mathbf{a}\| \cdot \|\mathbf{c}\|}, & v_B &= \pm \frac{n_1 l_2 - l_1 n_2}{2 \cdot \|\mathbf{a}\| \cdot \|\mathbf{c}\|}, & w_B &= \pm \frac{l_1 m_2 - l_2 m_1}{2 \cdot \|\mathbf{a}\| \cdot \|\mathbf{c}\|}, \\ u_C &= \pm \frac{l_1 - l_2}{2 \cdot \|\mathbf{c}\|}, & v_C &= \pm \frac{m_1 - m_2}{2 \cdot \|\mathbf{c}\|}, & w_C &= \pm \frac{n_1 - n_2}{2 \cdot \|\mathbf{c}\|}, \end{aligned} \right\} \quad (16)$$

where Eqs. (16) also follows from (14) and (15) and represent new exact formulas to estimate of the direction cosines of the principal axes \bar{A} ($\mathbf{a} = \mathbf{a}(u_A, v_A, w_A)$), \bar{B} ($\mathbf{b} = \mathbf{b}(u_B, v_B, w_B)$), and \bar{C} ($\mathbf{c} = \mathbf{c}(u_C, v_C, w_C)$). The direction cosines (l_1, m_1, n_1) of \mathbf{h}_1 and (l_2, m_2, n_2) of \mathbf{h}_2 are derived from the coefficients C_{2m}, S_{2m} according to (Marchenko, 1998).

Earth time-dependent mechanical and geometrical parameters

After the determination of the long-term contribution of $d\bar{A}_{20}(t)$ we get the time-dependent $H_D(t)$ based on Eq. (8). Fig. 3 shows this change in $H_D(t)$ based on $d\bar{A}_{20}(t)$ taken here as Solution II in Table 1. With $\bar{C}_{2m}(t), \bar{S}_{2m}(t),$ and $H_D(t)$ via the solution of the eigenvalue-eigenvector problem we come to the Earth's mechanical and geometrical parameters.

The time-dependent coefficients $\bar{C}_{2m}(t), \bar{S}_{2m}(t)$ were extracted for the following time series: a) 1976-2020; b) 1992-2011; c) GSR Release 06 (2011-2020) taken from UT/CSR (<https://www.csr.utexas.edu/datasets/ftp-portal-grace-data/>). These $\bar{C}_{2m}(t), \bar{S}_{2m}(t)$ with a step size from weekly to monthly solutions were applied for the

computation of the temporally varying Earth's mechanical and geometrical parameters.

Table 2 shows remarkable stability in the time of the axes \bar{A} and \bar{B} due to small deviations in latitude and longitude ($345.067^\circ \div 345.075^\circ$), ($75.067^\circ \div 75.075^\circ$), respectively, during the period from 1992 to 2020 (see, also Marchenko, 2009a).

Because of a great number of various parameters (twenty) computed for every t we give here only mean values of some time-dependent quantities obtained by averaging their instant values. These average values of the Earth's time-dependent mechanical and geometric parameters and their uncertainties during the time-interval from 1992.844640 yr to 2020.371 yr. are shown in Table 3.

Table 2

Average values of the spherical coordinates of the principal axes computed via Eq. (16) and given in the accepted ITRF system. Their estimates at epoch $t_0 = 2000$ are given in brackets

Axis	Latitude [degree]	Longitude [degree]
\bar{A}	-0.0000430 (-0.0000451)	345.07094 (345.07084)
\bar{B}	0.0000921 (0.0000940)	75.070941 (75.070836)
\bar{C}	89.999898 (89.999895)	280.16230 (280.67896)

Table 3

Average values of the Earth's time-dependent mechanical and geometric parameter and their uncertainties during the time-interval from 1992.8 yr to 2020.4 yr. ($GM = 398600.4415 \text{ km}^3\text{s}^{-2}$; $a = 6378136.3 \text{ m}$; epoch $t_0 = 2000$; zero frequency tide system)

Parameter	Mean value	Minimum	Maximum
1	2	3	4
$\bar{A}_{20} \cdot 10^{-6}$	$(-484.169561653 \pm 0.000014)$	-484.170060986	-484.169132852
$\bar{A}_{22} \cdot 10^{-6}$	$(2.812636730 \pm 0.00019)$	2.812117252	2.812997518
H_D	$0.0032737951 \pm 0.0000000005$	0.0032737944	0.0032737956
A	$0.32961129 \pm 0.00000005$	0.32961104	0.32961159
B	$0.32961855 \pm 0.00000005$	0.32961830	0.32961885
C	$0.33069756 \pm 0.00000005$	0.33069731	0.33069786
$I_m = \frac{A+B+C}{3}$	$0.32997580 \pm 0.00000005$	0.329975551	0.329976102
p_A	50.28812427	50.28700040	50.28884813
$(C - A) \cdot 10^6$	$(1086.26715090 \pm 0.00025)$	1086.2659601	1086.2683628

Cont. Table 3

1	2	3	4
$(C - B) \cdot 10^6$	$(1079.00495408 \pm 0.00025)$	1079.0038943	1079.0059753
$(B - A) \cdot 10^6$	$(7.26219681 \pm 0.000012)$	7.26085552	7.26312836
$\alpha = (C - B) / A$	$(3273.567947 \pm 0.005) \cdot 10^{-6}$	3273.566265	3273.569255
$\beta = (C - A) / B$	$(3295.527948 \pm 0.005) \cdot 10^{-6}$	3295.525205	3295.529757
$\gamma = (B - A) / C$	$(21.960237 \pm 0.0015) \cdot 10^{-6}$	21.956187	21.963055
$1/f$	298.2564416 ± 0.00001	298.256292	298.256570
$1/f_e$	91437.107 ± 6.1	91425.380	91453.9980
$M_2 \cdot 10^{-6}$	$(1086.26715090 \pm 0.00025)$	1086.2659601	1086.2683628
$\tilde{\gamma}$ [in degree]	$170^\circ.619988 \pm 0.000005$	$170^\circ.619387$	$170^\circ.6208506$
$(C - B)/(C - A)$	$0.9933145389 \pm 0.0000004$	0.9933136846	0.9933157663
$(B - A)/(C - A)$	$0.006685461124 \pm 0.000005$	0.0066842337	0.0066863154

Then, determining parameters connected with $\dot{\bar{A}}_{20} = -0.7461 \cdot 10^{-11} \text{ yr}^{-1}$ (Table 1, Solution III), the linear dependence $\delta F(t) = \dot{F}(t - t_0)$, where $\dot{F} = \frac{dF(t)}{dt}$ is chosen at epoch t_0 , some changes in the frame of the linear model $\delta F(t) = \dot{F}(t - t_0)$

during the period 27.5 years (from 1992 to 2020) are given in Table 4, assuming the parameter $q = const$. Table 3 and Table 4 contain the coefficients α , β , γ of the Euler dynamic equations (Moritz and Muller, 1987), the polar f and equatorial f_e flattening, and their long-term variations.

Table 4

Long-term variations in some astronomical and geodetic parameters based on the long-wavelength drift in the coefficients $\bar{A}_{20} \approx \bar{C}_{20}$ and \bar{A}_{22} ($t_0 = 2000$)

Parameter	Long-term variation $\dot{F} = \frac{dF}{dt}$
1	2
$\bar{A}_{20} \approx \bar{C}_{20}$	$\dot{\bar{A}}_{20} = -0.7461 \cdot 10^{-11} \text{ yr}^{-1}$
\bar{A}_{22}	$\dot{\bar{A}}_{22} = 0.4316 \cdot 10^{-11} \text{ yr}^{-1}$
H_D	$\dot{H}_D = -\sqrt{5} \dot{\bar{A}}_{20} \frac{\text{Trace}(\mathbf{I})}{3C^2} = 5.0339 \cdot 10^{-11} \text{ yr}^{-1}$
p_A	$\dot{p}_A = \dot{H}_D \frac{\delta H_D}{\delta p_A} = 0.023 \text{ "/cy}^2$
A	$\dot{A} = \sqrt{5} \dot{\bar{A}}_{20} = -1.668 \cdot 10^{-11} \text{ yr}^{-1}$
B	$\dot{B} = \sqrt{5} \dot{\bar{A}}_{20} = -1.668 \cdot 10^{-11} \text{ yr}^{-1}$
C	$\dot{C} = -2\sqrt{5} \dot{\bar{A}}_{20} = 3.337 \cdot 10^{-11} \text{ yr}^{-1}$

Cont. Table 4

1	2
$\alpha = \frac{C-B}{A}$	$\dot{\alpha} = -\frac{\sqrt{5}\dot{A}_{20}(C-B+3A)}{3A^2} = 5.067 \cdot 10^{-11} \text{ yr}^{-1}$
$\beta = \frac{C-A}{B}$	$\dot{\beta} = -\frac{\sqrt{5}\dot{A}_{20}(C-A+3B)}{3B^2} = 5.067 \cdot 10^{-11} \text{ yr}^{-1}$
$\gamma = \frac{B-A}{C}$	$\dot{\gamma} = \frac{\sqrt{5}\dot{A}_{20}(B-A)}{3C^2} = -3.692 \cdot 10^{-16} \text{ yr}^{-1}$
$\sigma_E = \frac{C-A}{A}\omega$	$\dot{\sigma}_E = \frac{\sqrt{5}\dot{A}_{20} \cdot (2A+C)}{3A^2}\omega = -5.0671 \cdot 10^{-11} \omega \text{ yr}^{-1}$
f	$\dot{f} = -\frac{3\sqrt{5}\dot{A}_{20}}{2} = 2.5025 \cdot 10^{-11} \text{ yr}^{-1}$
f_e	$\dot{f}_e = \sqrt{15}\dot{A}_{22} = 1.6718 \cdot 10^{-11} \text{ yr}^{-1}$

Among the parameters from Table 4 all long-term changes have the same order as variation \dot{A}_{20} excluding $\dot{\gamma}$ and \dot{p}_A . According to Williams (1994) the variation \dot{p}_A called also \dot{J}_2 precession rate with the range $(-11.6 \text{ to } -16.8) \times 10^{-3} ["/\text{cy}^2]$ is dependent on the adopted $\dot{J}_2 = -\sqrt{5}\dot{C}_{20}$. Williams' \dot{J}_2 precession rate $\dot{p}_A = -0.014 ["/\text{cy}^2]$ given in 1994 corresponds to $\dot{C}_{20} = 1.3416 \cdot 10^{-11} \text{ yr}^{-1}$ and differs from those of Table 4 because of the opposite sign and the value $\dot{p}_A = 0.023 ["/\text{cy}^2]$. It should be noted that a large anomaly in the time-series of \bar{C}_{20} was detected by Cox and Chao (2002). Such anomaly leads to a jump about 1998 and the change of the \bar{C}_{20} sign during 1998–2002 years (see Fig.1). By this, we get an opposite sign concerning Williams' results and other parameters given in Table 4 (see also, Marchenko, 2009a). Thus, this new value $\dot{p}_A = 0.023 ["/\text{cy}^2]$ requires additional treatment given by the Earth's rotation theory which is outside the scope of this paper.

Thus, significant values over 50–100 years in the change of the parameters from Table 4, including the variation $\dot{\sigma}_E$ in the Euler frequency σ_E are rather unclear. It can be explained by various behaviors with time of their linear drift including the change of a sign of different effects. The accuracy of these parameters has similar or lower values as the uncertainty of

H_D . Consequently, the average values $\dot{\alpha}$ and $\dot{\beta}$ can be involved in the precession-nutation theory, taking into account the general theory (Moritz and Muller, 1987) for the time-varying Earth.

3D density distribution corresponding to the time-varying Earth's inertia tensor

Determination of the planet's density distribution $\delta(\rho, \vartheta, \lambda)$ from the external gravitational potential of the planet requires a solution of the famous inverse problem of the Newtonian potential. Hereafter ρ is the relative distance ($0 \leq \rho \leq 1$) from the origin to an internal current point; ϑ and λ are the polar distance and longitude of this point. If the planet's gravitational potential energy E (Rubincam, 1979; Moritz, 1990; Marchenko, 2009b) and the density at the surface are known as additional information, this problem transforms from an improperly posed (according to Hadamar) to a properly posed (as stated by Tikhonov) problem with its possible solution for the three-dimensional density distribution through the 3D Cartesian moments (Mescheryakov, 1991).

In this study we prefer to use A_{20} , A_{22} , and additional information about dynamical ellipticity H_D for the model of the 3D global density distribution $\delta(\rho, \vartheta, \lambda)$. It was derived by Mescheryakov and Deineka (1977) and modified by Marchenko (2009b) for the Earth, having a shape of the ellipsoid of revolution with the polar flattening f and the semi-major axis a . This model represents the exact (restricted by the order 2) solution of the 3D Cartesian

moments problem for $\delta(\rho, \vartheta, \lambda)$ in the following form

$$\delta(\rho, \vartheta, \lambda) = \delta(\rho)_R + \Delta\delta(\rho, \vartheta, \lambda), \quad (17)$$

$$\Delta\delta(\rho, \vartheta, \lambda) = \Delta K + \rho^2 (\Delta K_1 \sin^2 \vartheta \cos^2 \lambda + \Delta K_2 \sin^2 \vartheta \sin^2 \lambda + \Delta K_3 \cos^2 \vartheta), \quad (18)$$

$$\left. \begin{aligned} \Delta K &= \frac{5}{4} \delta_m [5\Delta I_{000} - 7(\Delta I_{200} + \Delta I_{020} + \frac{\Delta I_{002}}{\chi^2})], \\ \Delta K_1 &= \frac{35}{4} \delta_m (3\Delta I_{200} + \Delta I_{020} + \frac{\Delta I_{002}}{\chi^2} - \Delta I_{000}), \\ \Delta K_2 &= \frac{35}{4} \delta_m (\Delta I_{200} + 3\Delta I_{020} + \frac{\Delta I_{002}}{\chi^2} - \Delta I_{000}), \\ \Delta K_3 &= \frac{35}{4} \delta_m (\Delta I_{200} + \Delta I_{020} + 3\frac{\Delta I_{002}}{\chi^2} - \Delta I_{000}), \end{aligned} \right\} \quad (19)$$

$$\left. \begin{aligned} \Delta I_{000} &= I_{000} - I_{000}^R, & \Delta I_{200} &= I_{200} - I_{200}^R, \\ \Delta I_{020} &= I_{020} - I_{020}^R, & \Delta I_{002} &= I_{002} - I_{002}^R. \end{aligned} \right\} \quad (20)$$

With $\chi = 1 - f$, mechanical parameters in Eqs. (19) are expressed through the dimensionless Cartesian moments of the density $\tilde{\delta}$ of a gravitating

where $\delta(\rho)_R$ is the piecewise reference radial density model with radial density jumps such as PREM (Dziewonski and Anderson, 1981):

body (see definition in Grafarend et al., 2000) restricted here by the order

$$n = p + q + r = 2$$

$$I_{pqr}(\delta) = \frac{1}{MR^n} \int_{\tau} x^p y^q z^r \cdot \delta(\rho, \vartheta, \lambda) \cdot d\tau, \quad (p + q + r = n), \quad (21)$$

where x, y, z are the Cartesian coordinates of the internal point; $d\tau$ is the volume element of the ellipsoid of revolution. I_{pqr} are values for $n = 2$ can

be computed through the Earth's mass and the dimensionless principal moments of inertia $A, B,$ and C expressed via Eq. (1):

$$I_{000} = 1, \quad I_{200} = \frac{B + C - A}{2}, \quad I_{020} = \frac{A - B + C}{2}, \quad I_{002} = \frac{A + B - C}{2}, \quad (22)$$

assuming ($I_{100} = I_{010} = I_{001} = 0$). The reference model $\delta(\rho)_R$ includes individual information about density jumps, the mean density δ_m^R , and the mean

moment of inertia I_m^R , which have been selected preliminary for the construction of the radial profile $\delta(\rho)_R$:

$$\left. \begin{aligned} I_{000}^R &= \frac{\delta_m^R}{\delta_m}, & I_{200}^R = I_{020}^R &= \frac{3I_m^R \delta_m^R}{2\delta_m (\chi^2 + 2)}, & I_{002}^R &= \frac{3 \cdot \chi^2 I_m^R \delta_m^R}{2 \cdot \delta_m (\chi^2 + 2)}, \\ \delta_m^R &= 3 \int_0^1 \delta(\rho)_R \rho^2 d\rho, & I_m^R &= \frac{2(\chi^2 + 2)}{3\delta_m^R} \int_0^1 \delta(\rho)_R \rho^4 d\rho. \end{aligned} \right\} \quad (23)$$

In contrast to Mescheryakov and Deineka, (1977) the moments $I_{000}^R, I_{200}^R, I_{020}^R,$ and I_{002}^R of the reference density $\delta(\rho)_R$ were derived for one common set of the convenient mean density δ_m and the mean moment of inertia I_m of the model (17) and density jumps entering into $\delta(\rho)_R$. Hence, this 3D global density [Eq.(17)] is

given in the principal axes system and agreed with the Earth's mass and the principal moments of inertia to conserve in this way the gravitational potential from zero to second degree, H_D , the geometrical flattening f , and density jumps. Fig. 4 demonstrates the density anomalies $\Delta\delta(\rho, \vartheta, \lambda)$ at the mantle/crust boundary ($r=6346.6$ km).

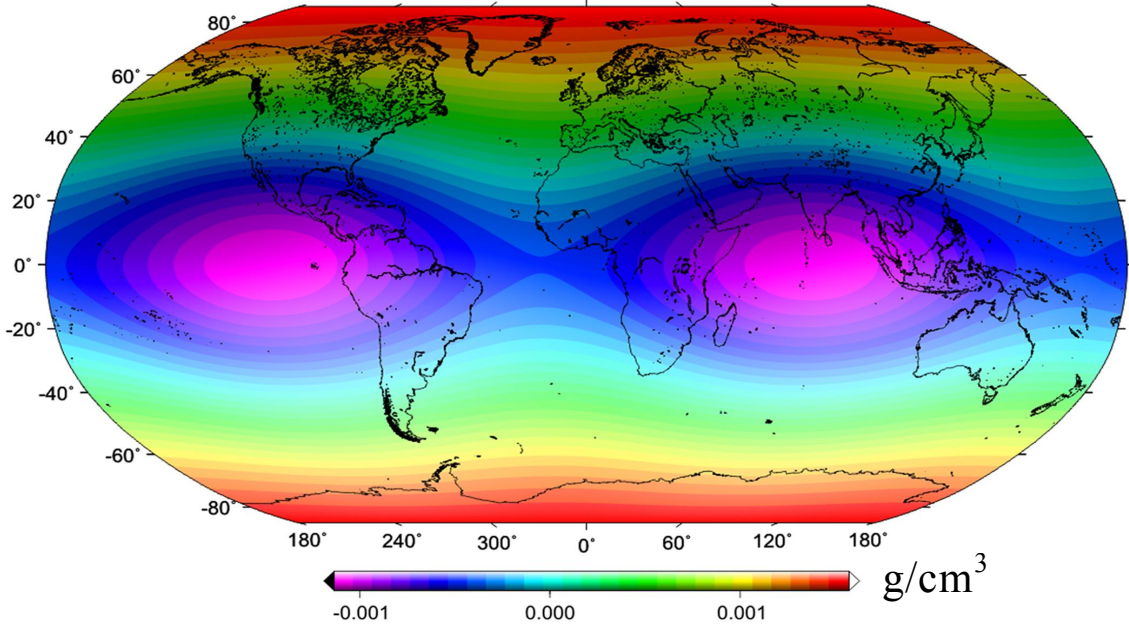


Fig. 4. Density anomalies [g/cm^3] $\Delta\delta(\rho, \vartheta, \lambda)$ at the mantle/crust boundary ($r=6346.6 \text{ km}$)

The radial density $\delta(\rho)_R$ is also treated within the ellipsoid of revolution if we use the formula $r_e = R(1 - 2f \cdot P_2(\cos\vartheta)/3)$ for the radius vector r_e (Moritz, 1990), where $P_2(\cos\vartheta)$ is the 2nd-degree Legendre polynomial. Eqs. (17)–(19) are

$$\tilde{r}_e = r \left[1 - \frac{2}{3} f \cdot P_2(\cos\vartheta) \right] \Rightarrow \rho = \frac{r}{R} = \frac{\tilde{r}_e}{r_e}. \quad (24)$$

By averaging $\delta(\rho, \vartheta, \lambda)$ over ellipsoidal surfaces we get the piecewise radial density as

$$\left. \begin{aligned} \delta(\rho) &= \delta(\rho)_R + [\Delta K + \rho^2 \Delta D] \\ \Delta D &= \frac{35}{12} \delta_m \left[5 \left(\Delta I_{200} + \Delta I_{020} + \frac{\Delta I_{002}}{\chi^2} \right) - 3 \Delta I_{000} \right] \end{aligned} \right\} \quad (25)$$

with the treatment of the reference density $\delta(\rho)_R$ inside the ellipsoidal Earth. Since the relative radius ρ is constant for each \tilde{r}_e , the radial densities $\delta(\rho)_R$ and $\delta(\rho)$ are also constant by Eqs. (25) at the ellipsoidal surface (24).

Then we remind that the adopted model (18) $\Delta\delta(\rho, \vartheta, \lambda)$ was derived from Eq. (19) and (22)

valid for a homothetic stratification when $f = \text{const}$ inside the ellipsoidal Earth. Therefore, if the set of the internal ellipsoidal surfaces \tilde{r}_e is labeled by the associated mean radius r of a sphere we have

where the principal moments of inertia $A(t)$, $B(t)$, $C(t)$ are time-dependent. Therefore the 4D term $\Delta'\delta(\rho, \vartheta, \lambda, t)$ with time-dependent parameters in Eq. (19) and Eq. (22) should be added to the 3D model $\Delta\delta(\rho, \vartheta, \lambda)$. From Eq. (22), Eq. (19) and Eqs. (1) we get

$$\Delta'K = \frac{35dC\delta_m}{4}, \quad \Delta'D = -\frac{175dC\delta_m}{12}, \quad \Delta'K_1 = \Delta'K_2 = \frac{35dC\delta_m}{2}, \quad \Delta'K_3 = \frac{35dC\delta_m}{4} \quad (26)$$

where dC is the time variation in the polar moment of inertia

$$dC = -\frac{2\sqrt{5}d\bar{A}_{20}(t)}{3} = -\frac{2\sqrt{5}}{3} \left(\dot{\bar{A}}_{20}(t-t_0) + \ddot{\bar{A}}_{20}(t-t_0)^2 \right), \quad (27)$$

taking into account Eq. (7). Substitution of Eq. (4), Eq. (7), and the sums $A(t) = A + dA$, $B(t) = B + dB$, $C(t) = C + dC$ (where A, B, C are the static components of the inertia tensor at epoch t_0) into the Eqs. (19)–(22) gives after simple

$$\delta(\rho, \vartheta, \lambda) = \delta(\rho)_R + \Delta\delta(\rho, \vartheta, \lambda) + \Delta'\delta(\rho, \vartheta, t), \quad (28)$$

$$\Delta'\delta(\rho, \vartheta, t) = \frac{35dC \cdot \delta_m}{4} [\rho^2(\sin^2 \vartheta + 1) - 1] = -\frac{35\sqrt{5}d\bar{A}_{20}(t) \cdot \delta_m}{6} [\rho^2(\sin^2 \vartheta + 1) - 1]. \quad (29)$$

In the case of the 1D density model given by Eqs. (25) we get

$$\delta(\rho) = \delta(\rho)_R + [\Delta K + \rho^2 \Delta D] + [\Delta'K + \rho^2 \Delta'D], \quad \Delta'D = \frac{35 \cdot \sqrt{5} d\bar{A}_{20} \cdot \delta_m}{6} [3 - 5\rho^2]. \quad (30)$$

All the five parameters $\Delta'K$, $\Delta'D$, $\Delta'K_1$, $\Delta'K_2$, and $\Delta'K_3$ have a direct dependence on dC and $d\bar{A}_{20}(t)$ based on (26). Hence by Eq. (26) and Eq. (25), we get after simple manipulations the time-dependent contribution $\Delta'\delta(\rho, \vartheta, t)$ in the form of (29) and (30) for these density models since the coordinate system $O\bar{A}\bar{B}\bar{C}$ is considered to be invariable. Here a dependence on the longitude λ is canceled but the time t is hidden in Eq. (27).

As the term $\Delta'K$ has a permanent influence on the entire Earth we prefer to use a relative element

$$\frac{\Delta'\tilde{\delta}}{\Delta'\tilde{\delta}_s} = \frac{\Delta'\tilde{\delta}_s(\rho, \vartheta, t)}{\Delta'\tilde{\delta}_s(\vartheta, t)} = \frac{\Delta'\tilde{\delta}(\rho, t)}{\Delta'\tilde{\delta}_s(t)} = \rho^2, \quad (\Rightarrow \Delta'\tilde{\delta} = \rho^2 \cdot \Delta'\tilde{\delta}_s), \quad (31)$$

where dependencies on ϑ and t are canceled. This parameter (31) expresses a relative characteristic of the density change along a radial profile. The quadratic function $\Delta'\tilde{\delta} / \Delta'\tilde{\delta}_s = \rho^2$ reflects the same permanent influence at epoch t independently of a considered radial profile and allows estimating the relative contribution of density changes in the frame of the model (31). Therefore, the mean values of this ratio (31) estimated inside the basic Earth's shells are (a) the crust – 99.6 %, (b) the upper mantle – 89.5 %, (c) the lower mantle – 52.9 %, (d) the outer core – 14.7 %, and (e) the inner core – 1.2 %. Thus, within the framework of the adopted model (28), (29) (except a permanent influence of $\Delta'K$) we come to a large amount of (31) inside the Earth's crust as the thinnest stratum of the planet that consists only of 0.4 % of the Earth's total mass.

Conclusions

Thus, the verification of approximate formulas for the modeling of the time-dependent astronomical dynamical ellipticity $H_D(t)$ fixed at epoch $t_0 = J2000$

algebra temporal changes in the parameters $\Delta'K$, $\Delta'D$, $\Delta'K_1$, $\Delta'K_2$, and $\Delta'K_3$ of the density model (17)–(18). As a result, Eqs. (17)–(18) for the 3D density distribution can be transformed to the following form

of the part $\Delta'\tilde{\delta}(\rho, \vartheta, t) = \Delta'\delta(\rho, \vartheta, t) - \Delta'K$ that corresponds to the Roche model $\Delta'\delta'(t) = \Delta'K + \rho^2 \Delta'D$ without $\Delta'K$. Obviously at the Earth's surface $\rho = 1$ the time-dependent function $\Delta'\tilde{\delta}$ will be independent of $0 \leq \rho \leq 1$. Then we introduce the auxiliary functions $\Delta'\tilde{\delta}_s(\vartheta, t) = \Delta'\tilde{\delta}_s(1, \vartheta, t)$, $\Delta'\tilde{\delta}_s(t) = \Delta'\tilde{\delta}_s(1, t)$ representing by (29) and (30) without $\Delta'K$.

Hence in both cases for the time-dependent density we get

($H_D = 3.27379448 \times 10^{-3}$) was provided by the additional estimation of each parameter of the Taylor series.

According to Maxwell (Maxwell, 1881), the potential (10) of gravitational quadrupole V_2 leads to the new exact formulas (16) for the orientation of the principal axes \bar{A} , \bar{B} , \bar{C} through the location of the two quadrupole axes \mathbf{h}_1 and \mathbf{h}_2 , always placed in the plane of the \bar{A} and \bar{C} axes.

The detection of the long-term variations $d\bar{A}_{20}$ was computed based on the UT/CSR solutions of $\bar{C}_{20}(t)$ during the time interval from 1976 to 2020. The basic model of the long-term variations from the UT/CSR solutions of $\bar{A}_{20}(t)$, $\bar{A}_{22}(t)$ during the time interval from 1992 to 2020 was revealed. Difference between \bar{C}_{20} and \bar{A}_{20} , given in various systems, has the value $\approx 2 \cdot 10^{-15}$ which is smaller than time changes in \bar{C}_{20} or \bar{A}_{20} . This characterizes the quality of the studied UT/CSR solutions.

Fundamental parameters of the Earth, including the principal axes and the principal moments of inertia were computed at each moment of t during 27.5 years. The linear changes in values of all considered 20 parameters are slightly unclear because of various behavior on different time-intervals, including variations of sign for these effects, due to a jump in the time-series $\overline{C}_{20}(t)$ during the time-period 1998–2002. For example, the Earth's polar flattening f increases within the second time-interval though Yoder (1983) and other authors have obtained the decreasing of f .

The Earth's 3D density model given by the restricted solution of the 3D Cartesian moments inside the ellipsoid of the revolution is based on the three principal moments of inertia as astronomic-geodetic information at each moment of t , including reference radial profile from seismic data treated as exact constituent. This model conserves the time-dependent gravitational potential from zero to second degree, the dynamical ellipticity, the polar flattening, basic radial jumps of density as sampled for the PREM model, and the long-term variations in space-time mass density distribution. It is important to note that in solving the inverse problem, the time dependence in the Earth's inertia tensor arises due to changes in the Earth's density but does not depend on changes in its shape, which is confirmed by Eq. (26) and Eq. (29) where flattening is canceled.

Acknowledgments. We would like to thank the Editors and the three anonymous reviewers for their significant comments, which led to improvements in the discussion of these results.

References

- Bourda, G., & Capitaine, N. (2004). Precession, nutation, and space geodetic determination of the Earth's variable gravity field. *Astronomy & Astrophysics*, 428(2), 691–702. DOI: 10.1051/0004-6361:20041533
- Bullard, E. C. (1954). The interior of the Earth. In: *The Earth as a Planet* (G. P. Kuiper, ed). Univ. of Chicago Press, 57–137.
- Bullen, K. E. (1975). *The Earth's Density*. Chapman and Hall, London.
- Burša, M., Groten E., & Šima, Z. (2008). Steady Change in Flattening of the Earth: The Precession Constant and its Long-term Variation. *The Astronomical Journal*, 135(3):1021–1023, doi.org/10.1088/0004-6256/135/3/1021
- Capitaine N., Wallace, P. T., & Chapront, J. (2003). Expressions for IAU 2000 precession quantities. *Astronomy & Astrophysics*, 412(2), 567–586. DOI: 10.1051/0004-6361:20031539
- Capitaine, N., Mathews, P. M., Dehant, V., Wallace, P. T., & Lambert, S. B. (2009). On the IAU 2000/2006 precession–nutation and comparison with other models and VLBI observations. *Celestial Mechanics and Dynamical Astronomy*, 103(2), 179–190, DOI 10.1007/s10569-008-9179-9
- Cheng, M. K., Eanes, R. J., Shum, C. K., Schutz, B. E., & Tapley, B. D. (1989). Temporal variations in low degree zonal harmonics from Starlette orbit analysis. *Geophysical Research Letters*, 16(5), 393–396.
- Chen, W., & Shen, W. (2010). New estimates of the inertia tensor and rotation of the triaxial nonrigid Earth. *Journal of Geophysical Research: Solid Earth*, 115: B12419. doi:10.1029/2009JB00709.
- Chen, W., Li, J. C., Ray, J., Shen, W. B., & Huang, C. L. (2015). Consistent estimates of the dynamic figure parameters of the earth. *Journal of Geodesy*, 89(2), 179–188. DOI 10.1007/s00190-014-0768-y
- Cheng, M., & Tapley, B. D. (2004). Variations in the Earth's oblateness during the past 28 years. *Journal of Geophysical Research: Solid Earth*, 109, B09402, doi:10.1029/2004JB003028, 2004
- Cheng, M., Ries, J. C., & Tapley, B. D. (2011). Variations of the Earth's figure axis from satellite *Research: Solid Earth*, 116. B01409, doi:10.1029/2010JB000850.
- Cheng, M., Tapley, B. D., & Ries, J. C. (2013). Deceleration in the Earth's oblateness. *Journal of Geophysical Research: Solid Earth*, 118(2), 740–747, doi:10.1002/jgrb.50058.
- Cheng, M., & Ries, J. (2017). The unexpected signal in GRACE estimates of C_{20} . *Journal of Geodesy*, 91(8), 897–914. DOI 10.1007/s00190-016-0995-5
- Cox, C. M., & Chao, B. F. (2002). Detection of a large-scale mass redistribution in the terrestrial system since 1998. *Science*, 297(5582), 831–833.
- Darwin, G. H. (1883). IV. On the figure of equilibrium of a planet of heterogeneous density. *Proceedings of the Royal Society of London*, 36 (228–231), 158–166.
- Dehant, V. et al. (1999) Considerations concerning the non-rigid Earth nutation theory. *Celestial Mechanics and Dynamical Astronomy*, 72, pp. 245–309.
- Dziewonski, A. M., & Anderson, D. L. (1981). Preliminary reference Earth model. *Physics of the earth and planetary interiors*, 25(4), 297–356.
- Fukushima, T. (2003). A new precession formula. *The Astronomical Journal*, 126(1), 494–534.
- Grafarend, E., Engels, J., & Varga, P. (2000). The temporal variation of the spherical and Cartesian multipoles of the gravity field: the generalized MacCullagh representation. *Journal of Geodesy*, 74(7–8), 519–530.
- Groten, E. (2004). Fundamental parameters and current (2004) best estimates of the parameters of common relevance to astronomy, geodesy, and geodynamics. *Journal of Geodesy*, 77, 724–797, doi:10.1007/s00190-003-0373-y
- IERS Standards (1989). (IERS Technical Note; 3). Chapter 14: Radiation Pressure Reflectance Model. Paris: Central Bureau of IERS-Observatoire de Paris.

- Liu, J. C., & Capitaine, N. (2017). Evaluation of a possible upgrade of the IAU 2006 precession. *Astronomy & Astrophysics*, 597, A83. DOI: 10.1051/0004-6361/201628717
- Lambeck, K. (1971). Determination of the Earth's pole of rotation from laser range observations to satellites. *Bulletin G od esique (1946–1975)*, 101(1), 263–281.
- Marchenko A.N. (1979) The gravitational quadrupole of a planet. Letters in Soviet Astronomical Journal, No. 5, 198–200.
- Marchenko A.N. (1998) *Parameterization of the Earth's gravity field. Point and line singularities*. Lviv Astronomical and Geodetic Society, Lviv.
- Marchenko, A. N. (2000). Earth's radial density profiles based on Gauss' and Roche's distributions. *Bollettino di Geodesia e Scienze Affini*, 59(3), 201–220.
- Marchenko, A. N., & Abrikosov, O. A. (2001). Evolution of the Earth's principal axes and moments of inertia: The canonical form of solution. *Journal of Geodesy*, 74(9), 655–669.
- Marchenko A. N. (2003) A note on the eigenvalue-eigenvector problem. In: Festschrift dedicated to Helmut Moritz on his 70th birthday. (Ed. N. K uhre ber) Institute for Geodesy, Graz University of Technology, Graz (Austria), pp. 143–152.
- Marchenko, A. N., & Schwintzer, P. (2003). Estimation of the Earth's tensor of inertia from recent global gravity field solutions. *Journal of geodesy*, 76(9–10), 495–509.
- Marchenko, A. N. (2009a). Current estimation of the Earth's mechanical and geometrical parameters. In: M. G. Sideris (ed.), *Observing our Changing Earth*. International Association of Geodesy Symposia 133. Springer-Verlag, Berlin, Heidelberg, pp. 473–481
- Marchenko A.N. (2009b) The Earth's global density distribution and gravitational potential energy. In: M. G. Sideris (ed.), *Observing our Changing Earth*, International Association of Geodesy Symposia 133. Springer-Verlag, Berlin, Heidelberg, pp. 483–491.
- Marchenko, A. N., & Lopushansky, A. N. (2018). Change in the Zonal Harmonic Coefficient C₂₀, Earth's Polar Flattening, and Dynamical Ellipticity from SLR Data. *Geodynamics*, 2(25), 5–14. (<http://dx.doi.org/10.4401/ag-7049>)
Published by Lviv Polytechnic National University. ISSN: 1992-142X (Print), 2519–2663 (Online), Lviv, Ukraine
- Mathews, P. M., Herring, T. A., & Buffett, B. A. (2002). Modeling of nutation and precession: New nutation series for nonrigid Earth and insights into the Earth's interior. *Journal of Geophysical Research: Solid Earth*, 107(B4), 10.1029/2001JB000390.
- Maxwell, J. K. (1881). *A Treatise on Electricity and Magnetism*. 2nd Edition, Oxford, Vol. 1, 179–214.
- Mescheryakov, G. A. (1991). Problems of the potential theory and generalized Earth. Nauka, Moscow, 203 p. (in Russian)
- Mescheryakov, G. A., & Deineka, J. P. (1977). A variant of the Earth's mechanical model. Geofysikalni Sbornik. XXV, Travaux de l'Inst. G ophysique de l'Acad emie Tch ecoslovaque des Science, No. 478, pp. 9–19.
- Moritz, H. (1990). *The Figure of the Earth. Theoretical Geodesy and Earth's Interior*, Wichmann, Karlsruhe.
- Moritz, H. & I. I. Muller (1987). *Earth Rotation. Theory and observation*, Ungar, New York.
- Melchior, P. (1978). *The tides of the planet Earth*. Pergamon.
- Petit, G., & Luzum, B (eds) (2010). *IERS conventions (2010)*, IERS Technical Notes 36. Observatoire de Paris, Paris.
- Rochester, M. G., & Smylie, D. E. (1974). On changes in the trace of the Earth's inertia tensor. *Journal of Geophysical Research*, 79(32), 4948–4951.
- Rubincam, D. P. (1984). Postglacial rebound observed by LAGEOS and the effective viscosity of the lower mantle. *Journal of Geophysical Research: Solid Earth*, 89(B2), 1077–1087.
- Schwintzer, P., Reigber, C., Massmann, F. H., Barth, W., Raimondo, J. C., Gerstl, M., ... & Lemoine, J. M. (1991). A new Earth gravity field model in support of ERS 1 and SPOT2: GRIM4-S1/C1, final report. *German Space Agency and French Space Agency., Munich/Toulouse*.
- Souchay, J., & Folgueira, M. (1998). The effect of zonal tides on the dynamical ellipticity of the Earth and its influence on the nutation. *Earth, Moon, and Planets*, 81(3), 201–216.
- Williams, J. G. (1994). Contributions to the Earth's obliquity rate, precession, and nutation. *The Astronomical Journal*, 108, 711–724.
- Yoder, C. F., Williams, J. G., Dickey, J. O., Schutz, B. E., Eanes, R. J., & Tapley, B. D. (1983). Secular variation of Earth's gravitational harmonic J₂ coefficient from Lageos and nontidal acceleration of Earth rotation. *Nature*, 303(5920), 757–762.

О. М. МАРЧЕНКО, С. С. ПЕРІЙ, З. Р. ТАРТАЧИНСЬКА, А. П. БАЛЯН

Національний університет “Львівська політехніка”, Інститут геодезії, вул. Карпінського, 6, Львів, 79013, Україна, march@pancha.lviv.ua, periy_ss@ukr.net, zrtartachynska@yahoo.com

ЧАСОВІ ЗМІНИ В ТЕНЗОРІ ІНЕРЦІЇ ЗЕМЛІ ТА 3D МОДЕЛЬ ГУСТИНИ НА ОСНОВІ ДАНИХ UT/CSR

Головною метою роботи є дослідження довгих часових рядів UT/CSR для коефіцієнтів гармонік другого ступеня $\bar{C}_{2m}(t)$, $\bar{S}_{2m}(t)$ гравітаційного поля Землі, отриманих за даними SLR. Якщо динамічна еліптичність $H_D(t)$ відома, вони дають змогу знаходити різні механічні та геометричні параметри Землі, що змінюється в часі, протягом таких періодів: (а) з 1976 до 2020 рр. на основі щомісячних та тижневих розв’язків коефіцієнта \bar{C}_{20} ; (б) з 1992 до 2020 рр. на основі щомісячних та тижневих розв’язків ненульових коефіцієнтів $\bar{A}_{20}(t)$, $\bar{A}_{22}(t)$, пов’язаних із системою головних осей інерції, що дає змогу будувати моделі їхніх довгострокових варіацій. Відмінності між \bar{C}_{20} і \bar{A}_{20} , заданими в різних системах, полягають у середньому значенні $\approx 2 \cdot 10^{-15}$, яке є меншим, ніж варіації у часі \bar{C}_{20} або \bar{A}_{20} , і характеризує високу якість рішень UT/CSR. Дві моделі залежної від часу динамічної еліптичності $H_D(t)$ побудовано з використанням довгострокових варіацій зонального коефіцієнта $\bar{A}_{20}(t)$ протягом останніх 44 та 27,5 року. Наближені формули для динамічної еліптичності $H_D(t)$, що залежить від часу, знайшли, додатково оцінивши кожен параметр ряду Тейлора і фіксуючи $H_D = 3.27379448 \times 10^{-3}$ на епоху $t_0 = J2000$ згідно з теорією прецесії-нутації IAU2000/2006. Потенціал залежного від часу гравітаційного квадруполя V_2 згідно із теорією Максвелла використано для виведення нових точних формул визначення орієнтації головних осей інерції \bar{A} , \bar{B} , \bar{C} через положення двох квадрупольних осей. Отже, залежні від часу механічні та геометричні параметри Землі, зокрема гравітаційний квадруполь, головні осі та головні моменти інерції, обчислювали у кожен момент часу протягом останніх 27,5 року з 1992 до 2020 рр. Однак їхня лінійна зміна у всіх розглянутих параметрах достатньо невизначена через різну поведінку на певних інтервалах часу, включаючи варіації знака різних ефектів через стрибок часових рядів $\bar{C}_{20}(t)$ протягом 1998–2002 рр. Моделі 3D та 1D густини Землі, задані обмеженим розв’язком 3D моментів густини всередині еліпсоїда обертання, отримано з умовами збереження залежного від часу гравітаційного потенціалу від нульового до другого степеня, динамічної еліптичності, полярного стиснення, основних радіальних стрибків густини, прийнятих для моделі PREM, і довгоперіодичної зміни в просторово-часовому розподілі густини планети. Важливо зазначити, що у разі розв’язування оберненої задачі залежність від часу в тензорі інерції Землі виникає внаслідок зміни густини Землі, але не залежить від змін її форми, про що свідчать відповідні рівняння, де стиснення скасовується.

Ключові слова: залежні від часу головні осі та моменти інерції Землі; динамічна еліптичність; гравітаційний квадруполь; теорія прецесії-нутації.

Received: 23.08.2020